

**Molecular dynamics study of a bilayer electron gas: Single particle properties**

S. Ranganathan

*Department of Physics, Royal Military College of Canada, Kingston, Ontario, Canada K7K 7B4*

R. E. Johnson

*Department of Mathematics and Computer Science, Royal Military College of Canada, Kingston, Ontario, Canada K7K 7B4*

(Received 21 October 2002; published 15 April 2003)

The single-particle dynamical properties of a strongly coupled, classical, symmetric electronic bilayer system have been investigated by molecular dynamics simulation. Results for the velocity correlation function, the single-particle scattering function, and their respective Fourier transforms have been calculated, and their behavior, as a function of the interlayer separation  $d$ , has been analyzed. The single-particle scattering function in particular, shows dramatic effects when the bilayer attains a staggered square lattice structure. This occurs when the interlayer separation is around  $0.8a$  ( $a$  is the Wigner-Seitz radius), where our previous study showed a marked decrease in the diffusion coefficient.

DOI: 10.1103/PhysRevE.67.041201

PACS number(s): 61.20.Ja, 61.20.Lc

**I. INTRODUCTION**

Charged particle bilayers have drawn considerable interest in the last decade, from both theoretical and experimental points of view. Such a system serves as a realistic model for charged particle traps, high- $T_c$  superconductors, and complex plasmas. It exhibits a variety of features that are due entirely to the interlayer Coulomb interactions. This system is characterized by two parameters: the plasma coupling constant  $\Gamma = e^2/ak_B T$  and the interlayer separation  $d$ ;  $a = (n\pi)^{-1/2}$  is the Wigner-Seitz (WS) radius with  $n$  the surface density of electrons,  $e$  the charge of the electron,  $k_B$  the Boltzmann constant, and  $T$  the temperature. The most remarkable feature on the static level is the diverse phase diagram of a classical bilayer Wigner crystal [1]. A Monte Carlo calculation [2] for the solid phases of a classical electronic bilayer with  $\Gamma = 196$  as a function of the interlayer separation confirms the sequence of distinct structural phases and its ranges as predicted by the lattice dynamics calculations of Goldoni and Peeters [1].

Recent molecular dynamics (MD) work [3,4] has shown that even in the liquid phase ( $\Gamma = 80$ , for example, for which the single-layer electron system is known to be well below its solid phase), a similar sequence of phase changes exists. Intralayer and interlayer pair correlation functions  $g_{11}(r)$  and  $g_{12}(r)$  for various values of  $\Gamma$  and  $d$  have been obtained. Although  $\Gamma = 80$  corresponds to a fluid phase of an isolated single-layer, two-dimensional electron gas system, the bilayer system portrays solidlike behavior in the pair correlation functions at intermediate values of  $d$ . In addition, MD results for self-diffusion [4] show a dramatic behavior: a decrease, by an order of magnitude, as the interlayer separation  $d/a$  is increased from 0 to 0.8, followed by a rapid increase which then levels off for  $d/a > 1.5$ .

However, very little research from a theoretical premise has been carried out on a classical bilayer one-component plasma, especially on its static and single-particle properties like diffusion. For example, calculations of pair correlation functions  $g_{11}(r)$  and  $g_{12}(r)$  and the corresponding static structure functions  $S_{11}(q)$  and  $S_{12}(q)$  using the hypernetted

chain technique [5] have yielded only fair agreement with MD results [3]. There are at least two hindrances to a theoretical development of the liquid phase dynamics of a classical charged particle bilayer: (i) a theoretical model normally requires, as input, interlayer and intralayer pair correlation functions, and (ii) there is a dearth of experimental and MD results with which to compare. The first impediment has been removed recently [3,4], and the object of this paper is to provide the needed MD results, at least those relating to single-particle dynamics. Computer simulations have provided a viable alternative to experiments, as they not only produce exact results for a given interparticle potential, but also allow us to calculate some basic properties that cannot be obtained from experiments. Previous MD results of mean-square displacement and self-diffusion [4] should help in formulating theoretical models of diffusion. In this paper, we provide MD results for the velocity correlation function  $\psi(t)$  and its transform  $Z(\omega)$ , and the self-intermediate scattering function  $F_s(q, t)$  and its transform  $S_s(q, \omega)$ , the self-density correlation function.

**II. SIMULATION TECHNIQUE**

The system to be simulated is a bilayer consisting of classical electrons interacting through a  $1/r$  Coulomb potential. The electrons are distributed evenly in two planes separated by a constant distance and are not allowed to move out of the planes. Charge neutrality is guaranteed by embedding the electrons in a uniform background of opposite charge. In each layer the basic simulation cell is a square, and periodic boundary conditions are imposed. A thermodynamic state of the system is entirely specified by the plasma coupling parameter  $\Gamma$  and the interlayer separation  $d$ . In what follows,  $d$  is expressed in units of  $a$ . Only symmetric bilayers, in which the density of the electrons is the same in both layers, are considered in this study. All quantities involved are in dimensionless units: distance in units of the WS radius  $a$ , and time in units of  $\tau = \sqrt{ma^3/e^2}$ , where  $m$  is the electron mass. The two layers have the same surface density and the basic cell is a square with side length  $L = (N/na^2)^{1/2}$ , containing

$N=128$  electrons in each of the two layers. Since  $a$  is the unit of length, the density in each layer takes the value  $1/\pi$ . This gives  $L=20.053$  in dimensionless units. The details of the simulation and of the extended Ewald sum technique used in our simulation were described in our previous papers [4,6].

After the equilibrium configuration has been achieved, the two-dimensional position and velocity components of each of the electrons in the two planes were computed and stored for 20 000 time steps, with the time step chosen to be 0.03. These components were then used to calculate the time correlation functions of interest. Note that the components for either layer must yield the same results.

The velocity correlation function (VCF), defined as  $\psi(t) = \langle \vec{v}_i(0) \circ \vec{v}_i(t) \rangle$  where  $\vec{v}_i(t)$  is the velocity of particle  $i$  in the lower layer (say) at time  $t$ , was computed using the formula

$$\psi(t) = \frac{1}{t_r} \frac{1}{N} \sum_{i=1}^N \sum_{t_0=1}^{t_r} [v_{xi}(t_0)v_{xi}(t_0+t) + v_{yi}(t_0)v_{yi}(t_0+t)], \quad (1)$$

where  $t_r$  is the number of time origins. The value of  $\psi(0)$ , in dimensionless units, is equal to  $2/\Gamma$  and thus provides a check on the accuracy of our calculations. We also calculated  $Z(\omega)$ , the Fourier transform of the normalized VCF  $\tilde{\psi}(t) \equiv \psi(t)/\psi(0)$ , given by

$$Z(\omega) = \frac{1}{2\pi} \int_{-\infty}^{\infty} \tilde{\psi}(t) e^{i\omega t} dt = \frac{1}{\pi} \int_0^{\infty} \tilde{\psi}(t) \cos(\omega t) dt, \quad (2)$$

and the diffusion coefficient  $D$ , as given by the Green-Kubo integral of the VCF

$$D = \frac{1}{2} \int_0^{\infty} \psi(t) dt = \frac{\pi}{\Gamma} Z(0). \quad (3)$$

The self-intermediate scattering function defined as

$$F_s(q, t) = \frac{1}{N} \left\langle \sum_{j=1}^N e^{i\vec{q} \cdot (\vec{r}_j(t) - \vec{r}_j(0))} \right\rangle \quad (4)$$

is computed using a similar formula to Eq. (1). The self-density correlation function is then computed using

$$S_s(q, \omega) = \frac{1}{2\pi} \int_{-\infty}^{\infty} F_s(q, t) e^{i\omega t} dt = \frac{1}{\pi} \int_0^{\infty} F_s(q, t) \cos(\omega t) dt. \quad (5)$$

### III. RESULTS AND DISCUSSION

We have calculated the VCF and the self-intermediate scattering function for various values of  $\Gamma$  and  $d$ . However, in this paper, we present the results and analysis for  $\Gamma=80$  only. This particular state is seen to exhibit a rich pattern of behavior, as seen from our earlier investigation [4]; it undergoes a sequence of structural phases and the diffusion coefficient changes dramatically as a function of the interlayer separation. For this value of  $\Gamma$ , the bilayer system behaves

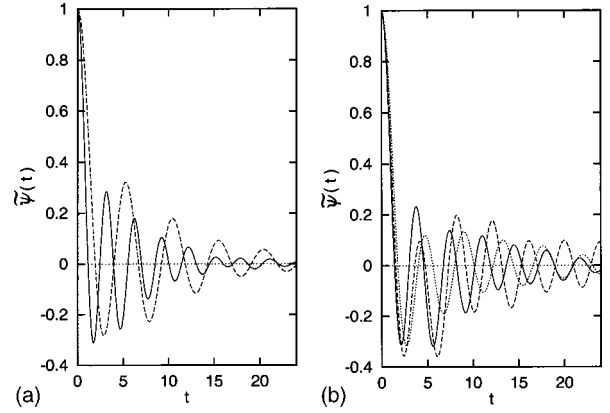


FIG. 1. (a) Normalized velocity correlation function as a function of time  $t$  (in units of  $\tau$ ) for  $\Gamma=80$ . Solid line is for  $d=0.1$  and dashed line for  $d=5.0$ . Interlayer separation  $d$  is in units of the Wigner-Seitz radius  $a$ . Quantities plotted in all figures are dimensionless. (b) Same as (a), except the solid line is for  $d=0.6$ , dashed for  $d=0.8$ , and dotted for  $d=1.1$ .

like a single-layer two-dimensional electron liquid for small ( $d < 0.1$ ) and large ( $d > 1.5$ ) interlayer separations, while for intermediate  $d$  it exhibits certain solidlike properties. Thus it would be of interest to see how the dynamics of a test particle is affected at this value of  $\Gamma$ , as a function of the interlayer separation.

#### A. Velocity correlation function

A very important probe of single-particle dynamics is provided by the velocity correlation function of a test particle. Since this quantity cannot be obtained experimentally, MD results become the sole source of comparison with predictions of any theoretical model.

In Fig. 1(a), we have plotted the normalized velocity correlation function as a function of time for  $\Gamma=80$ . The interlayer separation  $d$  is 0.1 (solid) and 5 (dashed). At these values of  $d$ , the bilayer should behave as an isolated single-layer, two-dimensional electron gas (2DEG). However, as  $d$  approaches 0, the two layers merge, thus doubling the density, reducing the WS radius  $a$  by a factor of  $\sqrt{2}$ , and increasing the value of  $\Gamma$  by the same factor. Thus the two graphs should agree with those of isolated single-layer, two-dimensional electron gas with  $\Gamma=113 (=80\sqrt{2})$  and 80, respectively. It has been shown that for a 2DEG the oscillation frequency is almost independent of  $\Gamma$ . Since our time abscissa is in terms of  $\tau$  (which involves  $\sqrt{a^3}$ ), we have to take into account a factor of  $2^{0.75} \approx 1.68$ , when comparing the two graphs. It is then seen that the frequencies of oscillation are essentially the same. The MD results on 2DEGs [7] show that the time period of oscillation is about 5.2 (in units of  $\tau$ ), in agreement with our results. It should also be noted that the peak heights decay in a very uniform manner.

In Fig. 1(b), we have plotted the normalized velocity correlation function for  $d=0.6, 0.8$ , and 1.1. The behavior of the VCF is quite different now. The peak positions and peak heights depend on the interlayer separation. The time period of oscillation decreases as  $d$  decreases and, in addition, the uniform decay of the peak height, evident in Fig. 1(a), is no

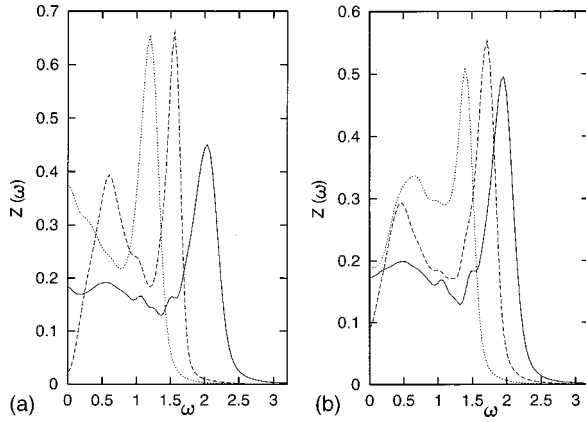


FIG. 2. (a) Fourier transform  $Z(\omega)$  (in units of  $\tau$ ) as a function of frequency  $\omega$  (in units of  $1/\tau$ ). Solid line is for  $d=0.1$ , dashed for  $d=0.8$ , and dotted for  $d=5.0$ . (b) Same as (a), except the solid line is for  $d=0.3$ , dashed for  $d=0.6$ , and dotted for  $d=1.1$ .

longer true, especially at short and intermediate times. The velocity correlations extend to much longer times, when compared to those of the 2DEG. These features should be attributed to the solidlike structural changes that take place in the bilayer for these values of interlayer separation.

It is of interest to see how these features show up in the frequency domain. In Fig. 2(a), we have plotted  $Z(\omega)$ , the frequency transform of the normalized VCF, as a function of  $\omega$  for  $d=0.1, 0.8$ , and  $5$ . Although the two graphs for  $d=0.1$  and  $5$  seem to be different, they are quite similar if we plot the normalized  $Z(\omega)$  and take into account the doubling of the density as  $d$  approaches  $0$ . For these values of  $d$ , there is only one side peak, the so-called plasmon peak, typical of a 2DEG. However, for  $d=0.8$  there are some distinct differences. The main peak is now much sharper (especially when compared to its value at zero frequency) and its position has also shifted. More importantly, we see that a second peak has emerged. The presence of the second peak has to be related to the solidlike behavior of a bilayer at such interlayer separations. In order to see the onset and disappearance of the double-peak feature, we have plotted  $Z(\omega)$  for  $d=0.3, 0.6$ , and  $1.1$  in Fig. 2(b). Our results show the second peak just starting to form at  $d=0.3$ , becoming sharper up to  $d=0.8$ , dropping off to a plateau at  $d=1.1$ , and disappearing completely around  $d=1.5$ . It is also interesting to note that the position of the second peak, which is around  $\omega=0.5$ , does not change appreciably with interlayer separation.

As a check on the accuracy of our calculations, we evaluated numerically the second-moment sum rule, given by

$$\Omega_0^2 = 2 \int_0^\infty \omega^2 Z(\omega) d\omega. \quad (6)$$

The exact expression given by the Einstein frequency appropriately generalized to a bilayer separated by distance  $d$  is

$$\Omega_0^2(d) = \frac{\pi n e^2}{m} \left[ \int_0^\infty \frac{1}{r^2} g_{11}(r) dr + \int_0^\infty \frac{r(r^2 - 2d^2)}{(r^2 + d^2)^{5/2}} g_{12}(r) dr \right], \quad (7)$$

where  $g_{11}(r)$  and  $g_{12}(r)$  are the intralayer and interlayer pair correlation functions. We evaluated Eq. (7) using our MD generated results for  $g_{11}(r)$  and  $g_{12}(r)$  [4]. The two integrals agree almost exactly for all values of  $d$ .

To see whether the double peak is a universal phenomenon for a bilayer, we calculated the VCF and the power spectrum for a lower value of the coupling constant. Similar plots of  $Z(\omega)$  for  $\Gamma=40$  do not reveal the existence of such a second peak for any value of interlayer separation. The criteria for a double peak in  $Z(\omega)$  then are a high value of the coupling constant  $\Gamma$  and intermediate values of the interlayer separation  $d$ . Previous MD studies on pair correlation functions [3,4] have shown the presence of crystalline phases for  $0.3 < d < 1.5$  for  $\Gamma=80$ . Hence one can relate the existence of a double peak in  $Z(\omega)$  to the structural phase changes of a strongly coupled bilayer. There is at present no theoretical model for the description of the VCF of a bilayer, and we hope our MD results will provide the motivation to attempt an explanation of the underlying mechanisms that are responsible for the double-peak feature in  $Z(\omega)$ . The plasmon peak in 2DEGs has been traced to the coupling between the single-particle motion and the collective modes. There exists an analogous situation in solids where the frequencies at the zone boundary manifest themselves strongly in the VCF. Thus a combination of these two effects would be needed to explain the double-peak phenomenon. It should also be noted that a double peak has been seen in a three-dimensional electron gas [8], but only for large values of  $\Gamma$  ( $>100$ ). We have also calculated the diffusion coefficient  $D$ , as given by Eq. (3), and compared it with our previously published results [4], which used the mean-square displacement definition; the agreement is very good.

## B. Single-particle scattering function

One of the basic quantities in any dynamical theory of fluids is the self-intermediate scattering function  $F_s(q, t)$ , defined in Eq. (4). Its frequency spectrum  $S_s(q, \omega)$ , defined in Eq. (5), has direct experimental relevance because of its connection to the incoherent part of the inelastic neutron scattering.

In Figs. 3(a)–3(d),  $F_s(q, t)$  is plotted as a function of  $t$  for various values of  $q$ . The value of the plasma parameter  $\Gamma$  is  $80$ , and the interlayer separations are  $d=0.1, 0.6, 0.8$ , and  $1.1$ , respectively. Recall that for small and large  $d$  the bilayer behaves very much like a single-layer 2DEG, but with  $\Gamma=80\sqrt{2}$  and  $80$ , respectively. Because of the periodic conditions imposed on the MD simulations, the values of  $q_x$  and  $q_y$  are limited to integral multiples of  $2\pi/L$  ( $=0.314$  in units of  $1/a$ ). We have limited our selection such that  $\vec{q}=(q_x, 0)$  and  $(0, q_y)$ . Since the system is in a fluid state for  $d=0.1$  and  $1.1$ , the behavior of  $F_s(q, t)$  is as expected; it starts from  $1$  and decays monotonically to  $0$  for large  $t$ , with the decay rate faster for larger  $q$ . However, for  $d$  near  $0.8$ , its behavior is strikingly different. For values of  $qa$  less than  $4$ ,  $F_s(q, t)$  has an initial rapid decay for small times ( $0 < t < 5$ ), followed by a pronounced plateau for intermediate times ( $20 < t < 60$ ). We have plotted these functions only up to  $t=100$ , to show these features clearly. There is a slow

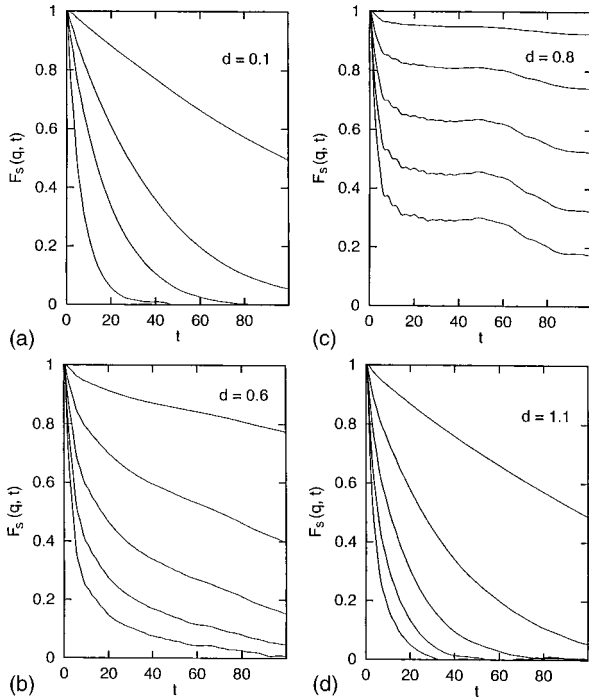


FIG. 3. Self-intermediate scattering function  $F_s(q, t)$  as a function of time  $t$  (in units of  $\tau$ ) for  $\Gamma = 80$ . The values of  $q$  (in units of  $1/a$ ) are, respectively, 0.94, 1.88, 2.82, 3.76, and 4.70 from top to bottom.  $d =$  (a) 0.1, (b) 0.6, (c) 0.8, and (d) 1.1.

decay to zero at larger times. For larger values of  $q$ , these features slowly disappear as we approach the ideal gas Gaussian behavior.

The behavior of  $F_s(q, t)$  for  $d = 0.8$ , is strikingly similar to that seen in MD simulations of compressed Lennard-Jones systems [9,10]. Such a decomposition into a fast and a slow decay has been attributed to a structural slowdown as the liquid is compressed to an amorphous state. Previous studies [4] indicate that, for this value of  $d$ , the diffusion coefficient is extremely small and is an order of magnitude less than that for the corresponding 2DEG. It has also been shown [3] that for  $\Gamma = 80$  the bilayer assumes a staggered square lattice structure at this value of  $d$ . Thus, our results for  $F_s(q, t)$  are

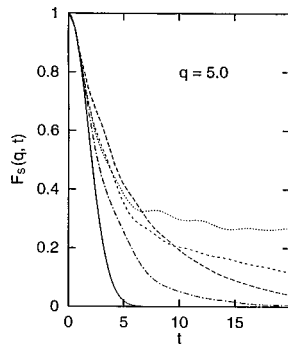


FIG. 4. Self-intermediate scattering function  $F_s(q, t)$  as a function of time  $t$  (in units of  $\tau$ ) for  $\Gamma = 80$  and  $q = 5.0$ . The ideal gas result is the solid line. The other lines are for  $d = 0.8, 0.6, 0.1$ , and  $1.75$ , respectively, from top to bottom on the right edge of the figure.

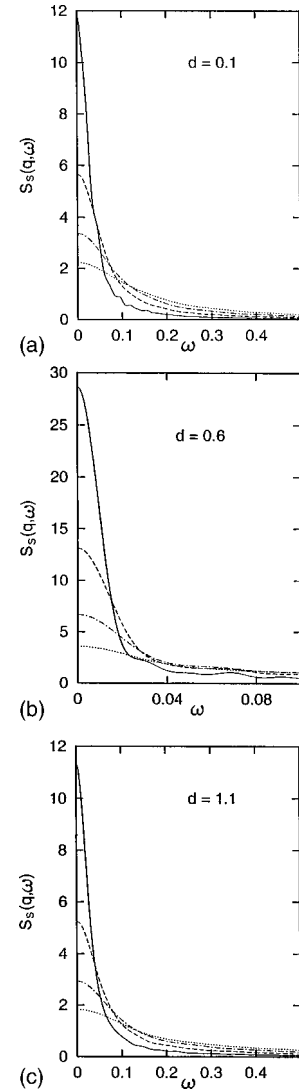


FIG. 5. Self-density correlation function  $S_s(q, \omega)$  (in units of  $\tau$ ), as a function of frequency  $\omega$  (in units of  $1/\tau$ ) for  $\Gamma = 80$ . The values of  $q$  (in units of  $1/a$ ) are, respectively, 1.88, 2.82, 3.76 and 4.70 from top to bottom on the left edge of the figure.  $d =$  (a) 0.1, (b) 0.6, and (c) 1.1.

consistent with other observed MD results and with theoretical findings which indicate that the square structure is the most stable among the structures that a bilayer undergoes as the interlayer separation is increased.

In order to illustrate how  $F_s(q, t)$  approaches ideal gas Gaussian values and to confirm its correct behavior for small  $t$ ,  $F_s(q, t)$  for a reasonably large value of  $qa$  ( $=5$ ) has been plotted in Fig. 4 for various values of interlayer separation  $d$ . As expected, the  $F_s(q, t)$  curves are closer to the ideal gas curve at small and large values of  $d$ , while the deviation is considerable for intermediate values of  $d$ . We need to go to still higher values of  $q$ , for these values of  $d$ , to approach the ideal gas behavior. Our results show that, for  $qa > 15$ ,  $F_s(q, t)$  values are very close to ideal gas values for all  $t$  and for all  $d$ .

In Figs. 5(a), 5(b), and 5(c) we have plotted  $S_s(q, \omega)$ , the Fourier transform of the intermediate scattering function

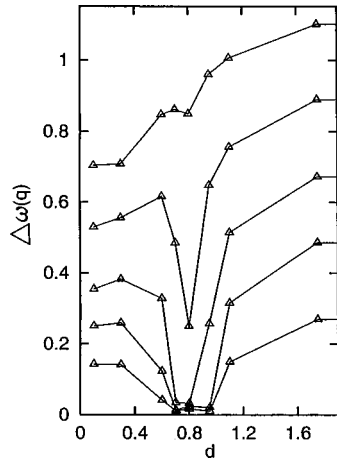


FIG. 6. Variation of  $\Delta\omega(q)$  (in units of  $1/\tau$ ), the half width at half maximum of  $S_s(q,\omega)$ , as a function of interlayer separation  $d$  (in units of  $a$ ) for  $\Gamma=80$  and  $q=4.70, 6.27, 7.53, 8.77,$  and  $10.04$  from bottom to top.

$F_s(q,t)$ , for some representative values of  $q$  and  $d$ . In all cases, there is a central peak, indicative of a diffusive process of the tagged particle. The very distinctive behavior of  $F_s(q,t)$  for  $d$  near 0.8 is masked in the Fourier transform and one sees a sharp central peak followed by a slow decay in  $S_s(q,\omega)$ .

Although one needs a full  $S_s(q,\omega)$  spectrum to compare any theoretical formulation with experimental or MD results, a considerable amount of information and a global picture can be obtained by plotting the half widths at half maximum (HWHM)  $\Delta\omega(q)$  and the peak heights  $S_s(q,0)$ . In order to see the effects of interlayer separations, we have plotted in Fig. 6 the variation of  $\Delta\omega(q)$  as a function of  $d$ , for a few fixed values of  $q$ . Figure 7 shows a plot of the peak height  $S_s(q,0)$  as a function of  $d$ . The lines in the graphs have been drawn only to serve as a guide to the eye. Both show a pronounced extremum around  $d=0.8$ , and they disappear slowly as  $q$  increases. For small and large  $d$ , where the system essentially behaves as a 2DEG,  $S_s(q,0)$  values are more or less the same, resulting in a nearly symmetrical plot. This is not seen to be true for  $\Delta\omega(q)$ .

For large  $q$ , the plotted quantities should approach ideal gas values, for any value of  $d$ . These are given by  $\Delta\omega(q) = \sqrt{[(2 \ln 2)/\Gamma]q}$  and  $S_s(q,0) = \sqrt{(\Gamma/2\pi)}1/q$ , in dimensionless units, and the plots would become a horizontal line. Although this is seen to be the case,  $S_s(q,0)$  approaches its ideal gas value faster than  $\Delta\omega(q)$ . In addition, the effect of  $d$  is more dramatic in the HWHM plot than it is in the peak height plot. The well in the HWHM becomes narrower as  $q$  increases, but the depth does not change significantly even

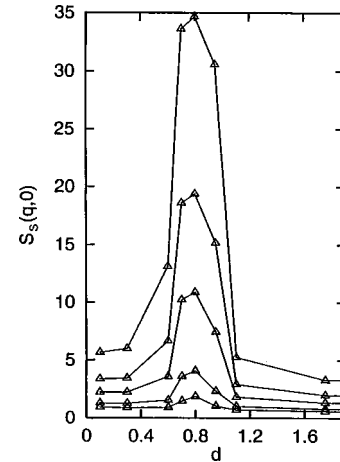


FIG. 7. Variation of  $S_s(q,0)$  (in units of  $\tau$ ) as a function of interlayer separation  $d$  (in units of  $a$ ) for  $\Gamma=80$  and  $q=2.82, 3.76, 4.70, 6.27,$  and  $7.53$  from top to bottom.

for  $qa=7.5$ . The sizable decrease in the HWHM at  $d\approx 0.8$  persists for a wide range of  $q$  values. These features again reinforce the conclusions drawn from previous results that the most dramatic changes in the properties of a bilayer occur when it is in the staggered square structural phase.

#### IV. SUMMARY

In this paper, we have reported results of molecular dynamics simulation of strongly coupled, classical symmetric electronic bilayers. The quantities that have been calculated and presented are the velocity correlation function, the single-particle intermediate scattering function, and their respective Fourier transforms. We have analyzed their variation as a function of the wave vector  $q$  and the interlayer separation  $d$ . These results, along with those published earlier, indicate a dominant crystalline structure at intermediate values of the interlayer separation; this staggered square structure is responsible for the dramatic changes seen in microscopic and macroscopic properties of a charged particle bilayer. Our results should provide an impetus to develop much needed theoretical models of charged particle bilayers. The predictions of the models can be tested against our MD results. MD results on collective properties of a bilayer, such as the full scattering function  $F(q,t)$  and its transform  $S(q,\omega)$ , will be the subject of a future paper.

#### ACKNOWLEDGMENT

This project was supported in part by a grant from the Academic Research Program (ARP) of the Department of National Defence, Canada.

- [1] G. Goldoni and F. M. Peeters, Phys. Rev. B **53**, 4591 (1996).  
 [2] J.-J. Weis, D. Levesque, and S. Jorge, Phys. Rev. B **63**, 045308 (2001).  
 [3] Z. Donkó and G. J. Kalman, Phys. Rev. E **63**, 061504 (2001).

- [4] S. Ranganathan, R. E. Johnson, and K. N. Pathak, Phys. Rev. E **65**, 051203 (2002).  
 [5] V. I. Valtchinov, G. J. Kalman, and K. B. Blagoev, Phys. Rev. E **56**, 4351 (1997).

- [6] R. E. Johnson and S. Ranganathan, Phys. Rev. E **63**, 056703 (2001).
- [7] J. P. Hansen, D. Levesque, and J.-J. Weis, Phys. Rev. Lett. **43**, 979 (1979).
- [8] J. P. Hansen, I. R. McDonald, and E. L. Pollock, Phys. Rev. A **11**, 1025 (1975).
- [9] J. Ullo and S. Yip, Phys. Rev. A **39**, 5877 (1989).
- [10] S. Ranganathan and G. S. Dubey, J. Phys.: Condens. Matter **5**, 387 (1993).